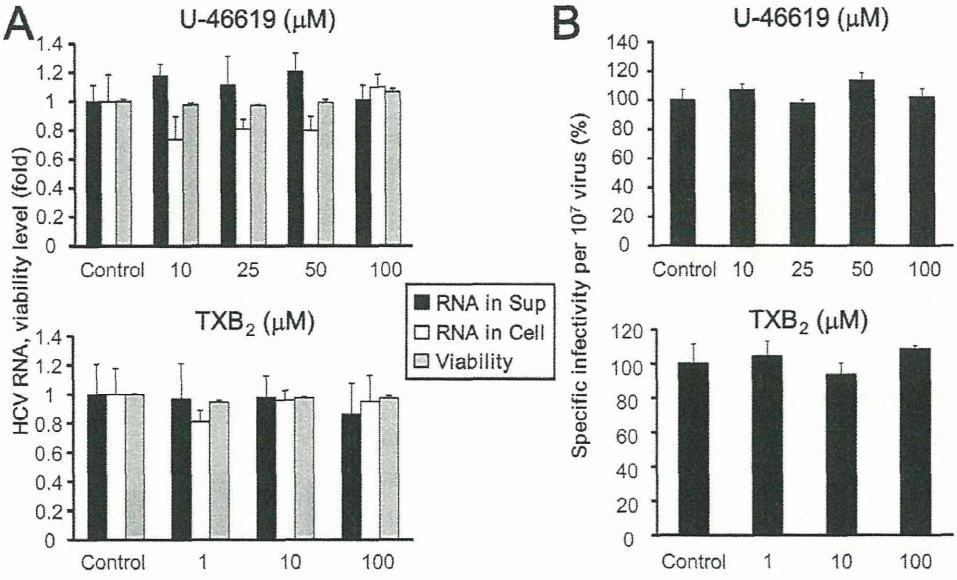


**Supplementary Figure 7.** Effects of U-46619 and $TXB_2$ on infectious HCV production. (*A*) Effects of U-46619 (*upper panel*) and $TXB_2$ (*lower panel*) on HCV-RNA levels in HCVcc-producing cell cultures. Levels of HCV RNA in the medium (*black bars*) and cells (*white bars*) treated with U-46619 or $TXB_2$ were assessed in qRT-PCRs and plotted as the amount relative to results observed with untreated cells (control). Mean cell viability ± SD for each sample condition also is plotted (*gray bars*). (*B*) Effects of U-46619 (*upper panel*) and $TXB_2$ (lower panel) on the infectivity of HCVcc produced in the cell-culture system were assessed.

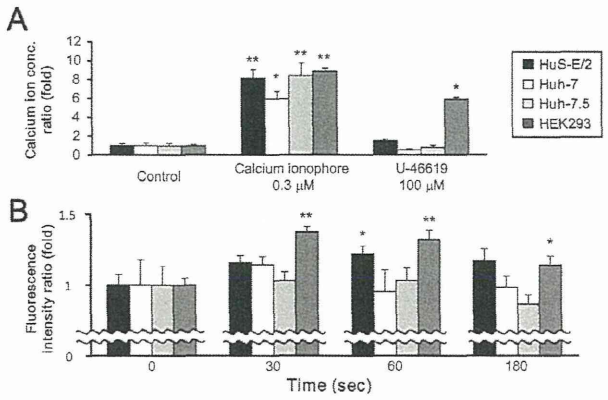


**Supplementary Figure 8.** Effects of U-46619 on HuS-E/2, Huh-7, Huh-7.5, and HEK293 cell lines via TP. (*A*) Concentrations of intracellular calcium ions were measured in HuS-E/2 (*black bars*), Huh-7 (*white bars*), Huh-7.5 (*gray bars*), and HEK293 (*dark gray bars*) cells treated with or without a calcium ionophore or U-46619. Calcium ion concentrations relative to those in mock-treated cells (control) were determined from triplicate wells in 2 independent experiments and are shown as means ± SD. (*B*) Actin polymerization after U-46619 treatment was measured with fluorescein isothiocyanate (FITC)-labeled phalloidin. *Differs from control, $P < .01$; **differs from control, $P < .001$.

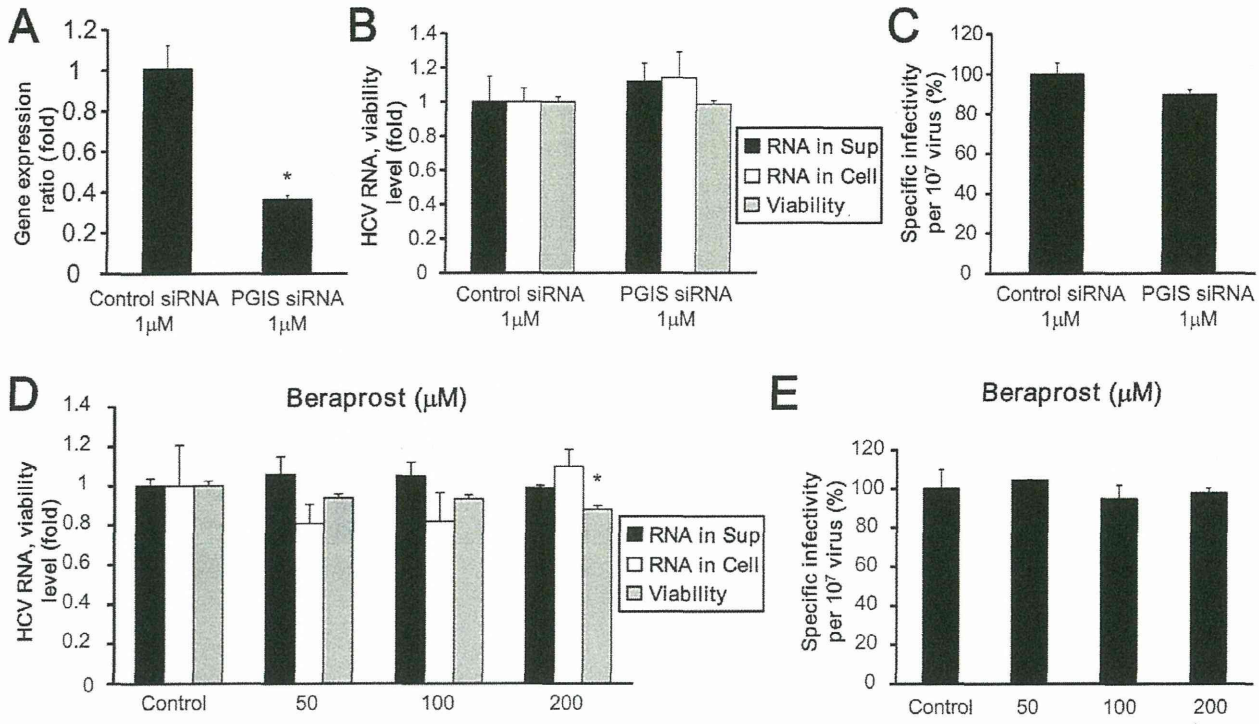


**Supplementary Figure 9.** Effects of $PGI_2$ on infectious HCV production. (*A*) siRNA-mediated knockdown of PGIS expression. (*B*) Effects of PGIS-specific siRNA on HCV-RNA levels in HCVcc-producing cell cultures. Levels of HCV RNA in medium (*black bars*) and cells (*white bars*) treated with control or PGIS-specific siRNA were assessed in qRT-PCR and are plotted as amounts relative to results obtained with control siRNA–treated cells (control). Mean cell viability ± SD for each sample condition also is plotted (*gray bars*). (*C*) Effects of PGIS-specific siRNA on the infectivity of HCVcc produced in the cell-culture system. (*D*) Effects of Beraprost on HCV-RNA levels in HCVcc-producing cell cultures. Levels of HCV RNA in medium (*black bars*) and HCVcc-producing Huh-7 cells (*white bars*) treated with Beraprost were assessed in qRT-PCRs and plotted as amounts relative to results obtained with untreated cells (control). Mean cell viability ± SD for each sample condition also is plotted (*gray bars*). (*E*) Effects of Beraprost on the infectivity of HCVcc in culture medium from HCVcc-producing cell cultures were assessed. *Differs from control, $P < .01$.

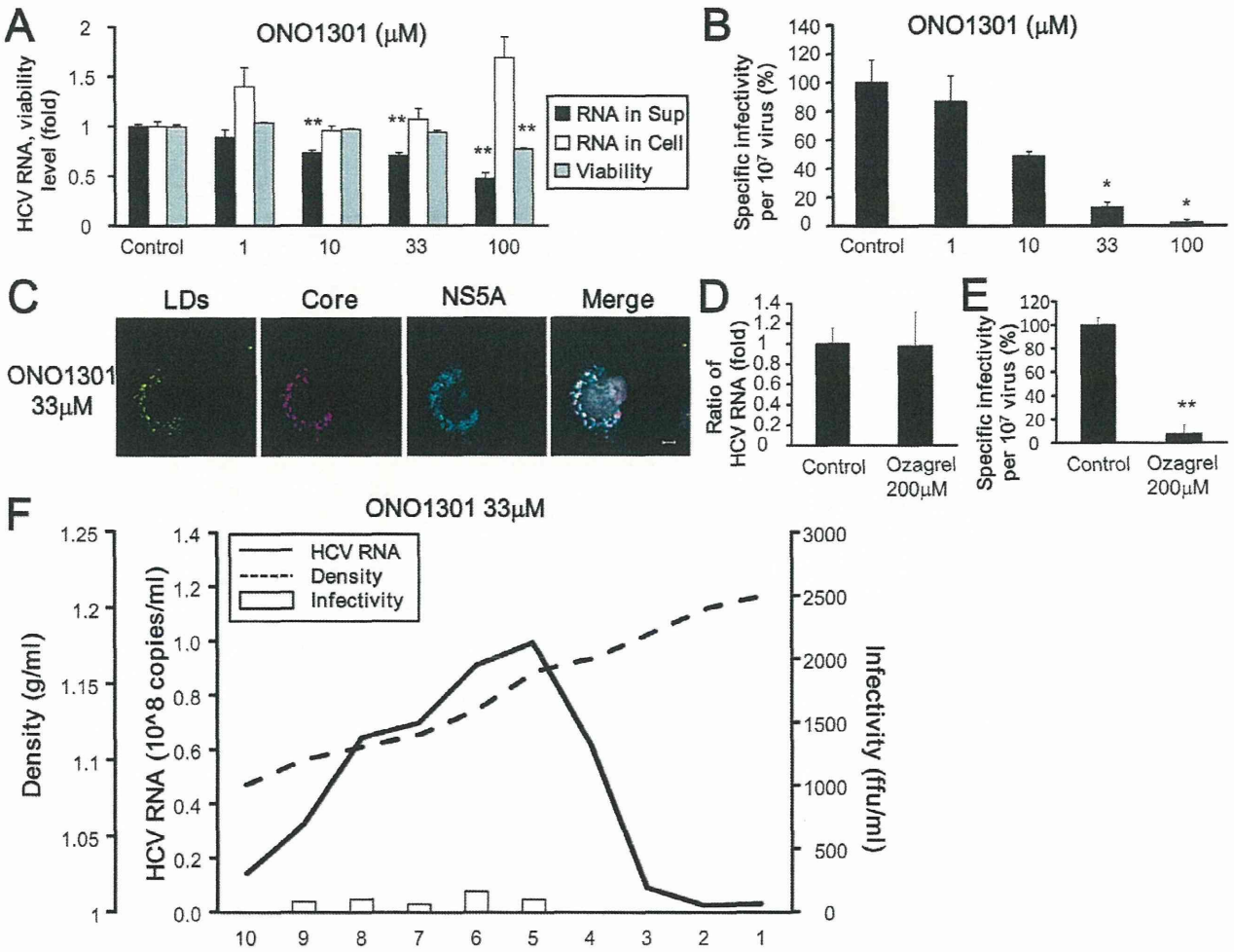


**Supplementary Figure 10.** Effects of ONO1301 on HCV lifecycle. (*A*) Levels of HCV RNA in medium (*black bars*) and cells (*white bars*) treated with or without ONO1301 were assessed. Mean cell viability ± SD for each sample condition also is plotted (*gray bars*). (*B*) The infectivity of HCVcc in culture medium from HCVcc-producing cell cultures treated with or without ONO1301 was assessed. (*C*) Subcellular locations of HCV core and NS5A proteins around LDs in the presence of ONO1301. Scale bars, 5 μm. (*D* and *E*) Levels and infectivity of intracellular HCV obtained from the cells treated with ONO1301. (*F*) Buoyant density of HCVcc obtained using cells treated with ONO1301. HCV RNA (*solid line*), fraction density (*dotted line*), and HCV infectivity (*white bars*) in each fraction collected by ultracentrifugation. *Differs from control, $P < .01$; **differs from control, $P < .001$.

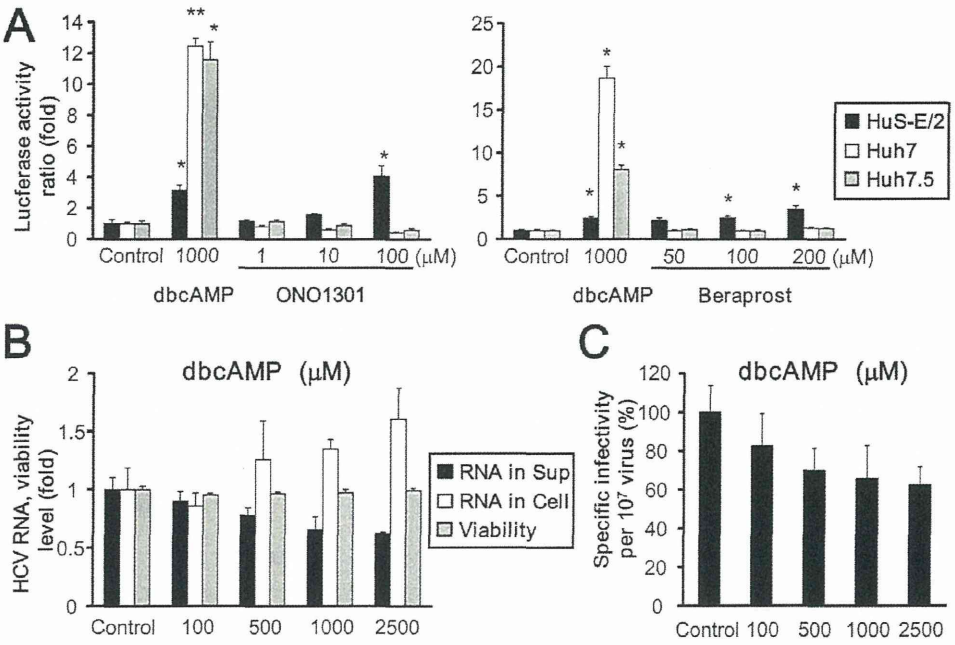


**Supplementary Figure 11.** Effects of dibutyryl cAMP (dbcAMP) on cell cultures producing JFH1 HCVcc. (*A*) HuS-E/2 (*black bars*), Huh-7 (*white bars*), and Huh-7.5 (*gray bars*) cells were transfected with CRE-Luc plasmid. Then, the luciferase activity in each sample was measured. Values were obtained from quadruplicate wells in 2 independent experiments and are shown as means ± SD. (*B*) Effects of dbcAMP on HCV-RNA levels in HCVcc-producing cell cultures. Levels of HCV RNA in medium (*black bars*) and cells treated with dbcAMP (*white bars*) were assessed in qRT-PCRs and plotted as amounts relative to results obtained with mock-treated cells (control). Mean cell viability ± SD for each sample condition also is plotted (*gray bars*). (*C*) Effects of dbcAMP on the infectivity of HCVcc produced using the cell-culture system. *Differs from control, $P < .01$; **differs from control, $P < .001$.

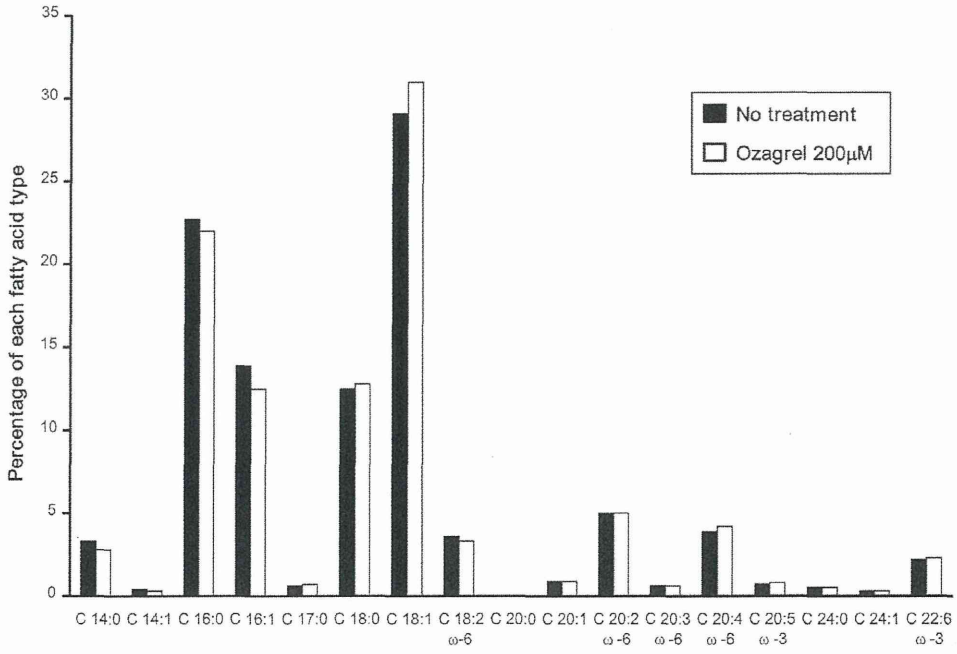


**Supplementary Figure 12.** Comparison of composition of fatty acids in HCV-infected Huh-7.5 cells with or without Ozagrel treatment.

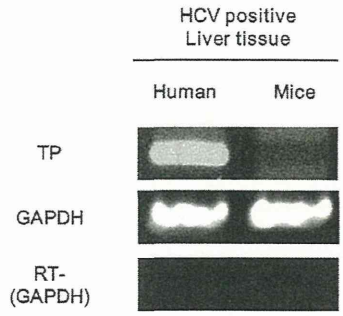


**Supplementary Figure 13.** Expression of TP mRNA in liver tissues from human patients and chimeric mice infected with HCV.

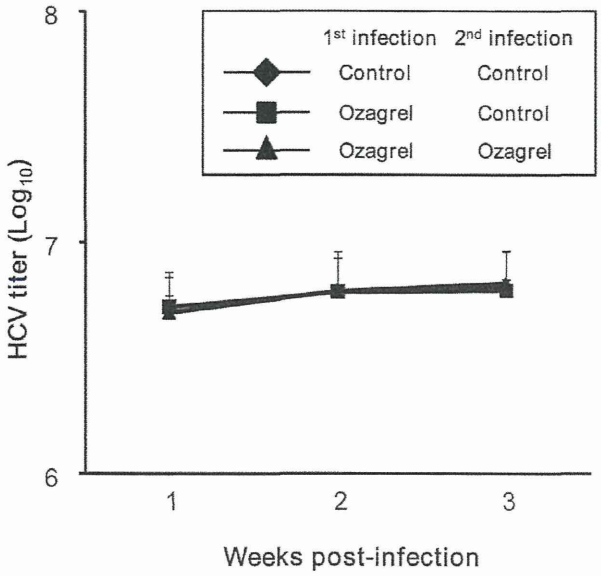


**Supplementary Figure 14.** Secondary infection of HCV derived from the chimeric mice model. Data are presented as means ± SD for 4 samples.

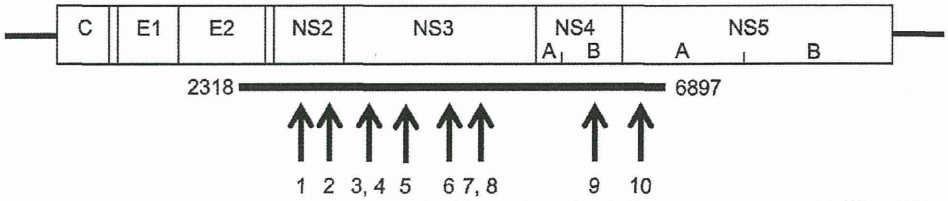


**Supplementary Figure 15.** Base substitutions in HCV genome collected from mice serum during a secondary infection. HCV genomic sequences from mice sera with Ozagrel treatment during primary and secondary infection was compared with those from mice without any treatment during both infection experiments. The region of obtained HCV genomic sequences is indicated (*thick bar*). The nucleotide positions of each base substitution are shown (*arrows*). Positions of base substitutions, and types of base substitution and amino acid replacement are listed in the *lower panel*.

| Number of substitution point | Position of nucleotide | Single base substitution | Amino acid replacement |
|---|---|---|---|
| 1 | 3192 | A→G | Asparagine→Aspartic acid |
| 2 | 3264 | A→G | Isoleucine→Valine |
| 3<br>4 | 3596<br>3597 | T→A<br>C→T | Phenylalanine→Tyrosine |
| 5 | 3859 | C→T | Serine→Leucine |
| 6 | 4283 | G→A | Methionine→Isoleucine |
| 7<br>8 | 4437<br>4439 | G→A<br>T→C | Glycine→Serine |
| 9 | 5886 | G→A | Valine→Methionine |
| 10 | 6747 | G→A | Alanine→Threonine |

**Supplementary Table 1.** Primer Sequences and Parameters in RT-PCR Experiments

| Genes | Primer Sequence 5′-3′ | Product size (bp) | Annealing Temperture | Cycle |
|---|---|---|---|---|
| COX1 | F: GCAGCTGAGTGGCTATTTCC | 324 | 60 | 32 |
| | R: ATCTCCCGAGACTCCCTGAT | | | |
| COX2 | F: GCAGTTGTTCCAGACAAGCA | 383 | 60 | 35 |
| | R: GGTCAATGGAAGCCTGTGAT | | | |
| PGES | F: GAAGAAGGCCTTTGCCAAC | 200 | 62 | 35 |
| | R: GGAAGACCAGGAAGTGCATC | | | |
| PGDS | F: AAGGCGGCGTTGTCCATGTGCAAGTC | 400 | 55 | 40 |
| | R: ATTGTTCCGTCATGCACTTATC | | | |
| PGIS | F: TCCTGGACCCACACTCCTAC | 395 | 60 | 40 |
| | R: GCGAAAGGTGTGGAAGACAT | | | |
| TXAS | F: TCTGCATCCCCAGACCTATC | 374 | 60 | 40 |
| | R: ATAGCCAGCGATGAGGAAGA | | | |
| GAPDH | F: ATGGGGAAGGTGAAGGTCGG | 250 | 60 | 40 |
| | R: TGGAGGGATCTCGCTCCTGG | | | |
| EP1 | F: GGTATCATGGTGGTGTCGTG | 324 | 60 | 40 |
| | R: GGCCTCTGGTTGTGCTTAGA | | | |
| EP2 | F: AGGAGAGGGGAAAGGGTGT | 267 | 60 | 40 |
| | R: TCTTAATGAAATCCGACAACAGAG | | | |
| EP3 | F: GACAGTCACCTTTTCCTGCAAC | 276 | 60 | 40 |
| | R: AGGCGAACAGCTATTAAGAAGAAG | | | |
| EP4 | F: CAGGACATCTGAGGGCTGAC | 269 | 60 | 40 |
| | R: GTAGAAGGTCGTCTCCTTCTGCTC | | | |
| DP | F: GCAACCTCTATGCGATGCAC | 292 | 60 | 32 |
| | R: GGGTCCACAATTGAAATCAC | | | |
| IP | F: AAGACTGGAGAGCCCAGACC | 161 | 60 | 40 |
| | R: CCACGAACATCAGGGTGCTG | | | |
| TP | F: CAGATGAGGTCTCTGAAGGTGTG | 304 | 60 | 40 |
| | R: CAGAGGAAGGTGAGGAAGGAG | | | |

NOTE. RT-PCRs were performed as follows: 25–40 cycles of 95°C for 30 seconds, 55–62°C for 30 seconds, and 72°C for 1 minute.

**Supplementary Table 2.** Primer Sequences and Parameters in qRT-PCR Experiments

| Genes | Primer Sequence 5′-3′ | Product Size (bp) |
|---|---|---|
| COX1 | F: TCCGGTTCTTGCTGTTCCTG | 151 |
| | R: TCACACTGGTAGCGGTCAAG | |
| PGES | F: CATCCTCTCCCTGGAAATCTCG | 129 |
| | R: CCGCTTCCTACTGTGACCC | |
| PGDS | F: CCTGTCCACCTTGCACAGTC | 123 |
| | R: TCATGCTTCGGTTCAGGACG | |
| PGIS | F: GCAGTGTCAAAAGTCGCCTG | 83 |
| | R: ACTCTCCAGCCATTTGCTCC | |
| TXAS | F: TTTGCTTGGTTGCCTGTTCC | 99 |
| | R: CCAGAGTGGTGGTCTTCCAG | |
| GAPDH | F: GACAGTCAGCCGCATCTTCT | 104 |
| | R: GCGCCCAATACGACCAAATC | |

NOTE. qRT-PCRs were performed as follows: 40 cycles of 95°C for 5 seconds, 60°C for 34 seconds.

OPEN ACCESS Freely available online

PLOS | ONE

# Cell Type-Specific Subcellular Localization of Phospho-TBK1 in Response to Cytoplasmic Viral DNA

**Takayuki Suzuki, Hiroyuki Oshiumi*, Moeko Miyashita¤a, Hussein Hassan Aly¤b, Misako Matsumoto, Tsukasa Seya***

Department of Microbiology and Immunology, Graduate School of Medicine, Hokkaido University, Sapporo, Hokkaido, Japan

## Abstract

Cytoplasmic viral RNA and DNA are recognized by RIG-I-like receptors and DNA sensors that include DAI, IFI16, DDX41, and cGAS. The RNA and DNA sensors evoke innate immune responses through the IPS-1 and STING adaptors. IPS-1 and STING activate TBK1 kinase. TBK1 is phosphorylated in its activation loop, leading to IRF3/7 activation and Type I interferon (IFN) production. IPS-1 and STING localize to the mitochondria and endoplasmic reticulum, respectively, whereas it is unclear where phosphorylated TBK1 is localized in response to cytoplasmic viral DNA. Here, we investigated phospho-TBK1 (p-TBK1) subcellular localization using a p-TBK1-specific antibody. Stimulation with vertebrate DNA by transfection increased p-TBK1 levels. Interestingly, stimulation-induced p-TBK1 exhibited mitochondrial localization in HeLa and HepG2 cells and colocalized with mitochondrial IPS-1 and MFN-1. Hepatitis B virus DNA stimulation or herpes simplex virus type-1 infection also induced p-TBK1 mitochondrial localization in HeLa cells, indicating that cytoplasmic viral DNA induces p-TBK1 mitochondrial localization in HeLa cells. In contrast, p-TBK1 did not show mitochondrial localization in RAW264.7, L929, or T-23 cells, and most of p-TBK1 colocalized with STING in response to cytoplasmic DNA in those mammalian cells, indicating cell type-specific localization of p-TBK1 in response to cytoplasmic viral DNA. A previous knockout study showed that mouse IPS-1 was dispensable for Type I IFN production in response to cytoplasmic DNA. However, we found that knockdown of *IPS-1* markedly reduced p-TBK1 levels in HeLa cells. Taken together, our data elucidated the cell type-specific subcellular localization of p-TBK1 and a cell type-specific role of IPS-1 in TBK1 activation in response to cytoplasmic viral DNA.

**Citation:** Suzuki T, Oshiumi H, Miyashita M, Aly HH, Matsumoto M, et al. (2013) Cell Type-Specific Subcellular Localization of Phospho-TBK1 in Response to Cytoplasmic Viral DNA. PLoS ONE 8(12): e83639. doi:10.1371/journal.pone.0083639

**Editor:** Haitao Guo, Drexel University College of Medicine, United States of America

**Received** August 12, 2013; **Accepted** November 5, 2013; **Published** December 9, 2013



**Funding:** This work was supported in part by grants-in-aid from the Ministry of Education, Science, and Culture of Japan, and the Ministry of Health Labor and Welfare of Japan, the Kato Memorial Bioscience Foundation, Yasuda Cancer Foundation, and the Ono Foundation. Financial supports by a MEXT Gran-in-Project "the Carcinogenic Spiral", the Natinal Cancer Center Research and Development Fund (23-A-44), and the Japan Initiative for Global Research Network on Infectious Disease (J-GRID) are gratefully acknowledged. The funders had no role in study design, data collection and analysis, decision to publish, or preparation of the manuscript.

**Competing interests:** The authors have declared that no competing interest exist.

* E-mail: oshiumi@med.hokudai.ac.jp (HO), seya-tu@pop.med.hokudai.ac.jp (T. Seya)

¤a Current address: Hokkaido Pharmaceutical University School of Pharmacy, Otaru, Hokkaido, Japan
¤b Current address: Department of Virology II, National Institute of Infectious Diseases, Shinjuku, Tokyo, Japan

## Introduction

RIG-I-like receptors (RLRs) are cytoplasmic viral RNA sensors that play an essential role in Type I interferon (IFN) expression in response to RNA virus infection [1]. RLRs recognize cytoplasmic double-stranded RNA (dsRNA) and the dsRNA analog polyI:C [1]. A recent study reported that RLRs localize on antiviral stress granules in response to cytoplasmic polyI:C or viral infection [2]. IPS-1 (also called MAVS, Cardif, and VISA) is a solo adaptor of RLRs and localizes on the outer-membrane of mitochondria and peroxisomes [3–7]. A recent study reported that a part of IPS-1 localizes on mitochondria-associated membranes (MAMs), which is a distinct membrane compartment that links the endoplasmic reticulum (ER) to the mitochondria [8]. RIG-I is then recruited to MAMs to bind IPS-1 [8]. There are several regulatory proteins on mitochondria such as MFN-1 and MFN-2 [9,10]. Association of RLRs with IPS-1 induces the formation of IPS-1 prion-like aggregates, leading to TBK1 activation [11] and consequent Type I IFN production [12,13]. Toll-like receptor 3 (TLR3) also recognizes viral dsRNA and polyI:C; however, TLR3 localizes to early endosomes or the cell surface and requires the adaptor TICAM-1 to induce Type I IFN expression [14–16].

Cytoplasmic DNA sensors, such as DAI, IFI16, DDX41, cGAS, and Mre11, recognizes DNA viruses [17–19]. These DNA sensors recognize not only viral DNA but also cytoplasmic

vertebrate or bacterial DNA [20,21]. RLRs are also involved in sensing cytoplasmic DNA [22,23]. Chen and colleagues have shown that DNA viruses can activate RIG-I pathway via RNA polymerase III [24]. Unlike RLRs, the DAI, IFI16, DDX41, and cGAS DNA sensors require the adaptor molecule STING to induce Type I IFN expression [19,25,26]. STING localizes to the ER and requires TBK1 to induce Type I IFN expression [19].

The protein kinase TBK1 is essential for Type I IFN expression in response to cytoplasmic DNA [27]. Ser-172 of TBK1 is autophosphorylated in its activation loop, and autophosphorylation is essential for triggering TBK1-dependent signaling [28]. Active TBK1 phosphorylates the transcription factor IRF-3, leading to relocalization of IRF-3 from cytoplasm to nucleus [29]. Recently, we showed that phospho-TBK1 (p-TBK1) localizes on mitochondria in response to cytoplasmic hepatitis C virus RNA [30]; however, it is unclear where TBK1 localizes in response to cytoplasmic viral DNA. Here, we used an anti-p-TBK1 specific antibody to determine the subcellular localization of p-TBK1 in response to cytoplasmic viral DNA. We elucidated the cell type-specific subcellular localization of p-TBK1 in response to cytoplasmic viral DNA.

## Results

### Localization of p-TBK1 on mitochondria in HeLa cells

We used anti-TBK1 (total TBK1) and anti-p-TBK1 antibodies to detect total TBK1 and p-TBK1 expression by western blotting and immunofluorescence microscopy analyses. Exogenous expression of RIG-I CARDs, TICAM-1, IPS-1, or STING induces the activation of downstream signaling without stimulation [4,14,26,31]. We found that exogenous expression of RIG-I CARDs, TICAM-1, IPS-1, or STING induced TBK1 phosphorylation, whereas total TBK1 levels were not affected (Figure 1A). We investigated the subcellular localization of p-TBK and total TBK1. Total TBK1 was dispersed through the cytoplasm, whereas p-TBK1 exhibited mitochondrial localization in HeLa cells that expressed RIG-I CARDs, IPS-1, or STING (Figure 1B and 1C). More than 70 % of p-TBK1 induced by RIG-I CARDs, IPS-1, or STING expression showed mitochondrial localization (Figure 1B). In contrast, p-TBK1 did not show mitochondrial localization in HeLa cells that expressed TICAM-1 (Figure 1B and 1C). These data suggested that the activation of RIG-I, IPS-1, or STING signaling, but not TICAM-1 signaling, induced p-TBK1 mitochondrial localization in HeLa cells.

Next, we examined the localization of p-TBK1 in HeLa cells after polyI:C or vertebrate dsDNA (salmon sperm DNA) stimulation. Previous studies reported that cytoplasmic vertebrate DNA induces Type I IFN expression [21,32]. When HeLa cells were stimulated with transfected polyI:C or dsDNA for 6 h, p-TBK1 levels increased (Figure 2A), and more than 80 % of p-TBK1 showed mitochondrial localization (Figure 2B and 2C). In contrast, when HeLa cells were stimulated with polyI:C without transfection to activate the TLR3 pathway, most of p-TBK1 did not localize on mitochondria (Figure 2B). These data indicated that p-TBK1 localized on mitochondria in response to cytoplasmic polyI:C or dsDNA but not to extracellular polyI:C.

Next, we compared the subcellular localization of p-TBK1 to other proteins after polyI:C transfection. We found that p-TBK1 colocalized with a mitochondrial protein MFN-1 (Figure 3A). In contrast, p-TBK1 barely colocalized with the stress granule marker G3BP (Figure 3A). To compare the p-TBK1 localization with IPS-1 and STING localizations, HA-tagged IPS-1 or FLAG-tagged STING were transfected into HeLa cells. At 24 h after transfection, cells were stimulated by mock or polyI:C transfection for 6 h. Although either IPS-1 or STING expression induced p-TBK1 staining without stimulation (Figure S1A and S1B), most p-TBK1 colocalized with HA-tagged IPS-1 but poorly colocalized with FLAG-tagged STING in both stimulated and mock-stimulated cells (Figure 3A and Figure S1). These data are consistent with previous observations that IPS-1, but not STING, is essential for Type I IFN production in response to polyI:C [6,25].

Next, we stimulated HeLa cells by dsDNA transfection. Interestingly, p-TBK1 colocalized with exogenously expressed HA-tagged IPS-1 (Figure 3B) in dsDNA stimulated HeLa cells, although IPS-1 is known to be dispensable for type I IFN production in response to DNA stimulation [33]. We found that p-TBK1 induced by DNA stimulation colocalized with a mitochondria marker MFN-1, and partially colocalized with a MAMs marker Presenilin-1 (PSEN-1) and exogenously expressed FLAG-tagged STING (Figure 3C-3E). Statistical analysis suggested that more than 60 % of p-TBK1 colocalized with HA-tagged IPS-1 and MFN-1, whereas less than 10 % of p-TBK1 colocalized with FLAG-tagged STING (Figure 3F). Approximately 30 % of p-TBK1 colocalized with PSEN-1 (Figure 3F). Taken together, these data suggested that most mitochondrial p-TBK1 induced by DNA transfection colocalized with IPS-1 and MFN-1 in HeLa cells. Because STING but not IPS-1 is essential for Type I IFN expression in response to cytoplasmic DNA [25,33], there appears to be an apparent contradiction between our subcellular localization and previous genetic data. Thus, we further focused on p-TBK1 localization induced by cytoplasmic DNA to dissect these apparently contradictory results.

### Cell Type-Specific Localization of p-TBK1 in Response to Cytoplasmic DNA

We investigated whether p-TBK1 induced by DNA transfection exhibited mitochondrial localization in other cell lines. As seen with HeLa cells, in HepG2 cells, p-TBK1 exhibited mitochondrial localization in response to cytoplasmic DNA (Figure 4A and 4F). In contrast, most p-TBK1 did not exhibit mitochondrial localization in L929, RAW264.7, a mouse hepatocyte cell line [34], or tree shrew fibroblast T-23 cells [35] (Figure 4B-4E). Statistical analysis showed that fewer than 20% of p-TBK1 localized on mitochondria in the mouse hepatocyte cell line, L929, RAW264.7, and tree shrew T-23 cells (Figure 4F). Although p-TBK1 colocalized with exogenously expressed HA-tagged IPS-1 but not FLAG-tagged STING in dsDNA stimulated HeLa cells (Figure 3B and 3C), most p-TBK1 colocalized with exogenously expressed FLAG-tagged STING in dsDNA stimulated L929, RAW264.7, mouse hepatocytes or T-23 cells but not in HepG2 (Figure 5A-5F).

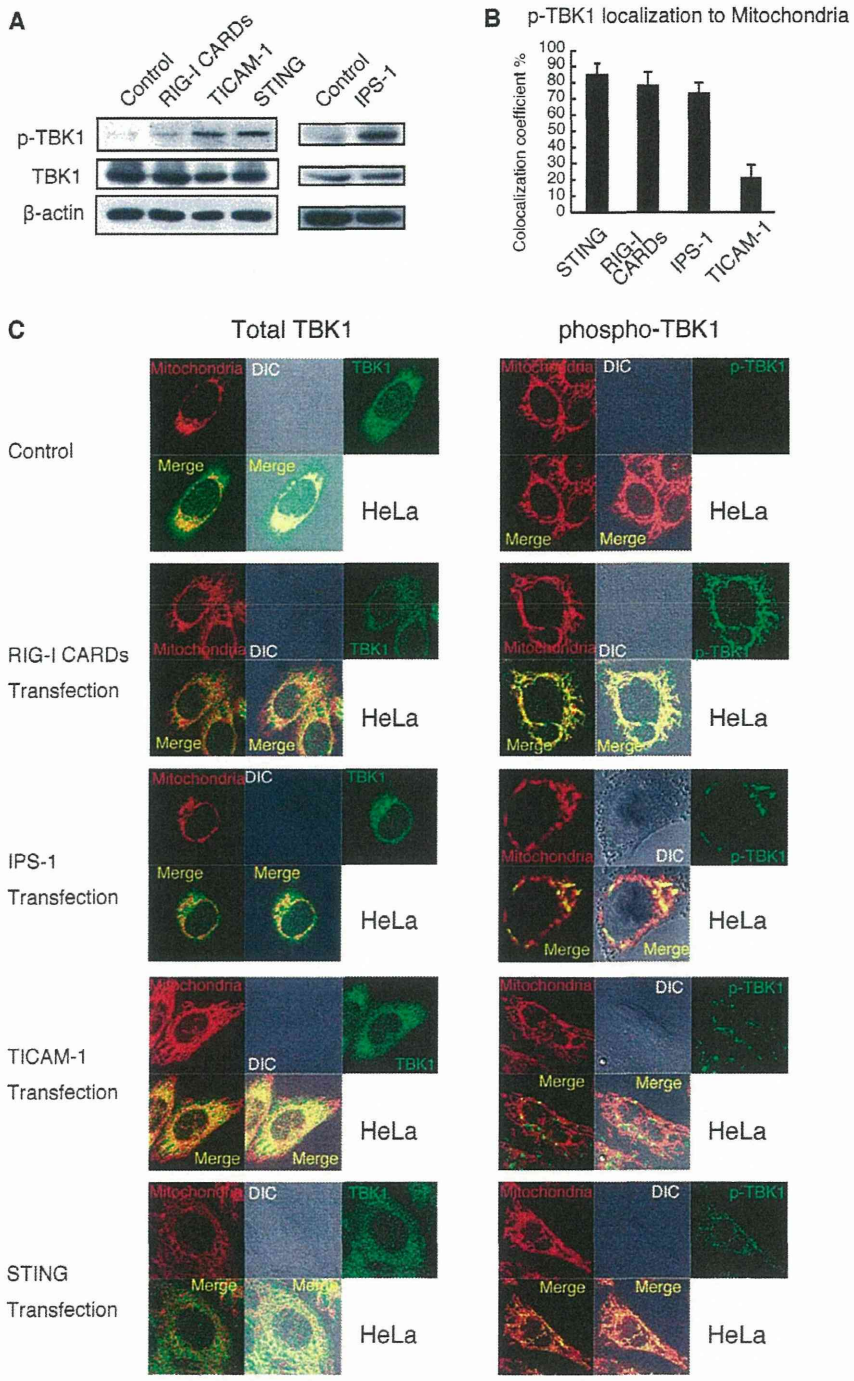


**Figure 1. Mitochondrial localization of p-TBK1 in HeLa cells.** (A) HeLa cells were transfected with 1.2 μg of empty vector, RIG-I CARDs, TICAM-1, IPS-1, or STING expression vectors in 6-well plate. At 24 h after transfection, cell lysates were prepared and subjected to SDS-PAGE. Proteins were detected by western blotting using anti-TBK1, p-TBK1, and β-actin antibodies.
(B and C) HeLa cells were transfected with 0.3 μg of empty vector or RIG-I CARDs, TICAM-1, or STING expression vectors in 24-well plate. At 24 h after transfection, cells were fixed and stained with anti-TBK1 or anti-p-TBK1 antibodies and Mitotracker Red. Colocalization coefficients of p-TBK1 with mitochondria were determined (mean ± sd, n = 3) (C). Unless otherwise indicated, Data are from one representative (n = 3) of at least three independent experiments.

doi: 10.1371/journal.pone.0083639.g001